

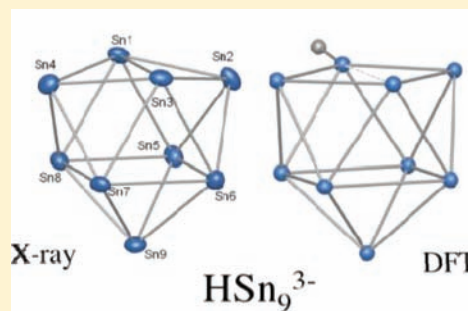
Surprising Acid/Base and Ion-Sequestration Chemistry of Sn_9^{4-} : HSn_9^{3-} , Ni@HSn_9^{3-} , and the Sn_9^{3-} Ion Revisited

F. Sanem Kocak, Domonique O. Downing, Peter Zavalij, Yiu-Fai Lam, Andrei N. Vedernikov, and Bryan Eichhorn*

Department of Chemistry and Biochemistry, University of Maryland, College Park, Maryland 20742, United States

S Supporting Information

ABSTRACT: K_4Sn_9 dissolves in ethylenediamine (en) to give equilibrium mixtures of the diamagnetic HSn_9^{3-} ion along with $\text{K}_x\text{Sn}_9^{(4-x)-}$ ion pairs, where $x = 0, 1, 2, 3$. The HSn_9^{3-} cluster is formed from the deprotonation of the en solvent and is the conjugate acid of Sn_9^{4-} . DFT studies show that the structure is quite similar to the known isoelectronic RSn_9^{3-} ions (e.g., $\text{R} = i\text{-Pr}$). The hydrogen atom of HSn_9^{3-} ($\delta = 6.18$ ppm) rapidly migrates among all nine Sn atoms in an intramolecular fashion; the Sn_9 core is also highly dynamic on the NMR time scale. The HSn_9^{3-} cluster reacts with $\text{Ni}(\text{cod})_2$ to give the Ni@HSn_9^{3-} ion containing a hydridic hydrogen ($\delta = -28.3$ ppm) that also scrambles across the Sn_9 cluster. The Sn_9^{4-} ion competes effectively with 2,2,2-crypt for binding K^+ in en solutions, and the pK_a of HSn_9^{3-} is similar to that of en (i.e., Sn_9^{4-} is a very strong Brønsted base with a pK_b comparable to that of the $\text{NH}_2\text{CH}_2\text{CH}_2\text{NH}^-$ anion). Competition studies show that the $\text{HSn}_9^{3-} \rightleftharpoons \text{Sn}_9^{4-} + \text{H}^+$ equilibrium is fully reversible. The HSn_9^{3-} anion is present in significant concentrations in en solutions containing 2,2,2-crypt, yet it has gone undetected for over 30 years.



INTRODUCTION

The Sn_9^{4-} Zintl ion was first prepared by Kraus¹ in 1907 but was not fully identified until the pioneering electrochemical studies by Zintl in the early 1930s.² Over 60 years later, the first crystal structure of the anion was reported in the low-resolution, partial structure of the $[\text{Na}(\text{en})_7]_4\text{Sn}_9$ solvent-shared ion pair (en = $\text{NH}_2\text{CH}_2\text{CH}_2\text{NH}_2$).³ Later, Corbett described⁴ the first fully resolved Sn_9^{4-} ion in the $[\text{Na}(2,2,2\text{-crypt})]_4\text{Sn}_9$ salt. The anion has a C_{4v} monocapped square antiprismatic structure (see I in Figure 1) and is characterized by multicenter bonding that has typically been described using Wade–Mingos electron counting rules.^{5,6} While there have been many derivatives of the Sn_9^{4-} ion described in the last 25 years, there are only two examples of crystallographically well-characterized “naked” Sn_9^{4-} ions: namely, Corbett’s $[\text{Na}(2,2,2\text{-crypt})]_4\text{Sn}_9$ salt and the more recent $[\text{Li}(\text{NH}_3)_4]_4\text{Sn}_9\cdot\text{NH}_3$ complex reported by Korber.⁷ To our knowledge, there are no examples of potassium (or rubidium or cesium) salts of naked Sn_9^{4-} reported.^{8,9} Instead, ethylenediamine (en) solutions of “ K_4Sn_9 ” in the presence of ion-sequestering agents give high yields of either cluster complexes containing direct $\text{K}^+\text{Sn}_9^{4-}$ contact ion pairs, such as $[\text{K}(2,2,2\text{-crypt})]_3\text{KSn}_9$,¹⁰ $[\text{K}(18\text{-crown-6})]_3\text{KSn}_9$, $[\text{K}(18\text{-crown-6})]_4\text{Sn}_9$,¹¹ and $[\text{K}(12\text{-crown-4})_2]_2[\text{K}(12\text{-crown-4})]_2[\text{Sn}_9]$,¹² or the well-known paramagnetic radical Sn_9^{3-} ions as the $[\text{K}(2,2,2\text{-crypt})]^+$ salts.^{13–17}

The Sn_9^{3-} ion was first reported in 1983¹³ and is now known in at least three different crystallographic modifications,^{14–17} which were all prepared from en solutions. While only sparingly soluble in en, the crystalline salts of Sn_9^{3-} are readily soluble in dmf and dmsO. In these solutions, the clusters give no

discernible ^{119}Sn NMR signals.^{13,18} In the solid state, EPR signals have been observed as well as bulk paramagnetism; however, the observed moments were less than expected from an $S = 1/2$ system.¹⁶

In this paper, we show that these solutions, and presumably the isolated salts, contain significant concentrations of the diamagnetic HSn_9^{3-} anion. The HSn_9^{3-} cluster is the conjugate acid of Sn_9^{4-} formed from the deprotonation of the en solvent. We show that the Sn_9^{4-} ion competes effectively with 2,2,2-crypt for binding K^+ in en solutions, and the pK_a of HSn_9^{3-} is similar to that of en (i.e., Sn_9^{4-} is a very strong Brønsted base with a pK_b comparable to that of the $\text{NH}_2\text{CH}_2\text{CH}_2\text{NH}^-$ anion). In solution, the hydrogen atom of HSn_9^{3-} rapidly migrates among all nine Sn atoms in an intramolecular fashion, and the Sn_9 core is also highly dynamic on the NMR time scale. The HSn_9^{3-} ion can also be metalated through reactions with $\text{Ni}(\text{cod})_2$ to give the Ni@HSn_9^{3-} ion in high yield. The HSn_9^{3-} anion is present in significant concentrations in en solutions containing 2,2,2-crypt, yet it has gone undetected for over 30 years. The unusual equilibrium properties and the highly dynamic nature of the clusters themselves have hindered full characterization of the HSn_9^{3-} ion in the past.

RESULTS

Synthesis. Melts of nominal composition “ K_4Sn_9 ” dissolved in en solutions containing 2,2,2-crypt (≥ 4 equiv) give very good yields ($>60\%$) of large brown $[\text{K}(2,2,2\text{-crypt})]_3\text{KSn}_9$.

Received: March 9, 2012

Published: April 29, 2012

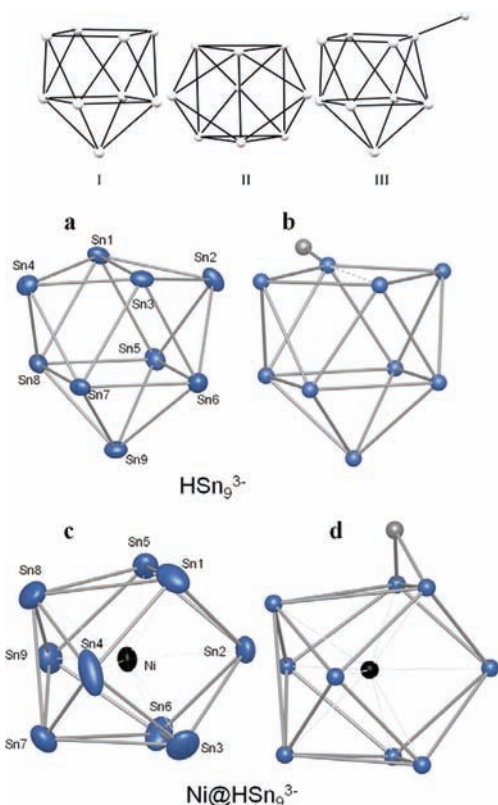
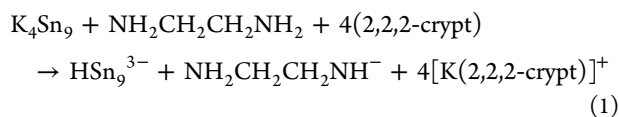


Figure 1. Structures I–III and ORTEP drawings of (a) the HSn_9^{3-} and (c) the Ni@HSn_9^{3-} ions. Thermal ellipsoids are drawn at the 50% probability level. The optimized DFT structures of HSn_9^{3-} and Ni@HSn_9^{3-} are shown in (b) and (d), respectively.

$\text{crypt}]]_3\text{HSn}_9 \cdot 1.5\text{en}$ crystals that contain the diamagnetic HSn_9^{3-} ion (eq 1). The crystals are soluble in dmf and dmsO and sparingly soluble in en. The HSn_9^{3-} ion is formed through an equilibrium process involving en and the Sn_9^{4-} ion, which is described in detail in the Equilibrium Studies section below.



Ethylenediamine solutions of HSn_9^{3-} react with excess $\text{Ni}(\text{cod})_2$ to give the Ni@HSn_9^{3-} ion as the $[\text{K}(2,2,2\text{-crypt})]^+$ salt according to eq 2.³⁰ The complex was isolated in high yield (ca. 71% yield) as a dark red crystalline solid. The Ni@HSn_9^{3-} ion cocrystallizes with the HSn_9^{3-} ion in ratios that vary with the $[\text{Ni}(\text{cod})_2]/\text{HSn}_9^{3-}$ ratio of the reaction. With excess $\text{Ni}(\text{cod})_2$, the Ni@HSn_9^{3-} ion is formed exclusively. The

$[\text{K}(2,2,2\text{-crypt})]_3\text{Ni@HSn}_9$ salt is soluble in py, dmf, and en. The HSn_9^{3-} and Ni@HSn_9^{3-} clusters have been characterized by single-crystal X-ray diffraction (XRD), ¹H and ¹¹⁹Sn NMR spectroscopy, and DFT calculations.



Structural Studies. The triclinic modification of the $[\text{K}(2,2,2\text{-crypt})]_3\text{HSn}_9 \cdot 1.5\text{en}$ salt is identical to the previously reported $[\text{K}(2,2,2\text{-crypt})]_3\text{Sn}_9 \cdot 1.5\text{en}$ salt (containing the Sn_9^{3-} ion) prepared by the exact same method.¹³ Details of the X-ray studies are given in the Supporting Information, and descriptions of the general crystallographic features of the previously reported Sn_9^{3-} ion can be found in refs 13–17. We describe here the structure of the HSn_9^{3-} ion, which is a reinterpretation of earlier findings and has not been previously presented.

The HSn_9^{3-} ion (Figure 1a) is a 22-electron 9-vertex *nido*-cluster and is isostructural to the RSn_9^{3-} ions^{19–21} (see III in Figure 1), where R = *t*-Bu, *i*-Pr. The structure is distorted away from that of the idealized C_{4v} monocapped square antiprism (see I) and is more similar to the D_{3h} tricapped trigonal prism (see II). Because the hydrogen atom could not be located crystallographically, DFT calculations were performed to locate the hydrogen position. Several independent calculations were performed with different starting cluster geometries and hydrogen atom locations. The lowest energy structure (Figure 1b) contains an Sn_9 core with an *exo* hydrogen attached to a single tin atom. These structural features are virtually identical to those in the RSn_9^{3-} ions (R = *t*-Bu, *i*-Pr).^{19–21} Comparisons of the DFT structures with the three known crystal structures are given in Table 1.

A comparison of calculated (DFT) structures for HSn_9^{3-} and the Sn_9^{3-} radical is given in Table 1 along with the crystallographic data for the three known crystallographic modifications of Sn_9^{3-} .^{13–15,17} The structures of the three $[\text{K}(2,2,2\text{-crypt})]_3\text{Sn}_9$ modifications are all quite similar, with only slight differences associated with crystal packing and lattice solvates. A summary of the crystallographic data for the three different modifications is given in Table 2. DFT calculations, all utilizing PBE functionals²² and two different program packages, Jaguar²³ and Priroda,^{24,25} were used in combination with several distinct basis sets. The root-mean-square (rms) differences in individual bond lengths between the DFT structures and the crystal structures of each known structure were determined (see Table 1). For reference, the DFT and experimental structures of the crystallographically unambiguous *i*-Pr Sn_9^{3-} cluster are given in column a as an illustration of the methods and basis sets. The results in column b show that all three methods can be used to distinguish the gas phase structures of the HSn_9^{3-} and Sn_9^{3-} clusters. The results given in

Table 1. Comparison of Crystallographic and Computational Structures of the Sn_9^{3-} and HSn_9^{3-} Ions

basis set ^b	rms differences (Å) in bond lengths of Sn_9 clusters ^a				
	XRD vs DFT: <i>i</i> -Pr Sn_9^{3-} column a	DFT: HSn_9^{3-} vs Sn_9^{3-} column b	XRD vs DFT for $\text{HSn}_9^{3-}/\text{Sn}_9^{3-}$		
			structure A column c	structure B column d	structure C column e
3z (Priroda)	0.088	0.148	0.164/0.081	0.120/0.111	0.113/0.116
cc-pVTZ-PP	0.103	0.137	0.159/0.088	0.122/0.117	0.117/0.121
LACV3P**++	0.152	0.143	0.199/0.149	0.171/0.171	0.166/0.173

^aFor structural details of *i*-Pr Sn_9^{3-} , see ref 20. Structure A, this work; structure B, ref 14; structure C, ref 15. ^bPriroda and Jaguar program packages (refs 23–25). See Supporting Information for details of basis sets and computational methods.

Table 2. Different Crystallographic Modifications of $\text{Sn}_9^{3-}/\text{HSn}_9^{3-}$

structure	space group	cell parameters	ref
$[\text{K}(2,2,2\text{-crypt})]_3[\text{Sn}_9]_{\text{en}_{1.5}}^a$	triclinic	$a = 15.002(1) \text{ \AA}$, $\alpha = 99.770(10)^\circ$ $b = 21.794(2) \text{ \AA}$, $\beta = 101.6(9)^\circ$ $c = 14.060(1) \text{ \AA}$, $\gamma = 89.694(10)^\circ$	13
$[\text{K}(2,2,2\text{-crypt})]_3[\text{Sn}_9]_{\text{en}_{0.5}}$	triclinic	$a = 14.896(3) \text{ \AA}$, $\alpha = 92.74(3)^\circ$ $b = 16.279(3) \text{ \AA}$, $\beta = 96.51(3)^\circ$ $c = 20.375(4) \text{ \AA}$, $\gamma = 111.81(3)^\circ$	15, 17
$[\text{K}(2,2,2\text{-crypt})]_6[\text{Sn}_9]_2\text{en}_{1.5}\text{tol}_{0.5}$	monoclinic	$a = 28.042(8) \text{ \AA}$ $b = 23.527(5) \text{ \AA}$, $\beta = 93.46(2)^\circ$ $c = 27.703(8) \text{ \AA}$	14
$[\text{K}(2,2,2\text{-crypt})]_3[\text{HSn}_9]_{\text{en}_{1.5}}$	triclinic	$a = 13.989(2) \text{ \AA}$, $\alpha = 89.391(1)^\circ$ $b = 14.889(2) \text{ \AA}$, $\beta = 79.589(2)^\circ$ $c = 22.004(2) \text{ \AA}$, $\gamma = 78.861(2)^\circ$	this work

^aNote that this cell can be transformed to the standard setting using $a' = c$, $b' = -a$, $c' = -b$ (0 0 1 / -1 0 0 / 0 -1 0) to give the standard cell: $a = 14.060 \text{ \AA}$, $b = 15.002 \text{ \AA}$, $c = 21.794 \text{ \AA}$, $\alpha = 89.69^\circ$, $\beta = 80.23^\circ$, $\gamma = 78.40^\circ$. The transformed cell is the same as the one reported here with slight variations presumably due to differences in temperature of data collection and perhaps partial solvation effects.

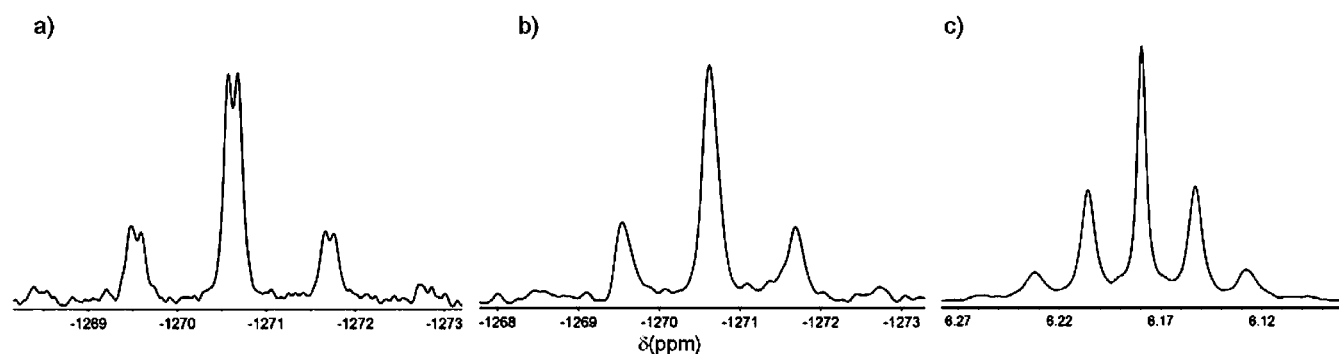


Figure 2. (a) ^{119}Sn NMR, (b) $\{^1\text{H}\}^{119}\text{Sn}$ NMR, and (c) ^1H NMR spectra of the HSn_9^{3-} ion. Data were recorded from a crystalline sample of the $[\text{K}(2,2,2\text{-crypt})]_3\text{HSn}_9\text{en}_{1.5}$ salt dissolved in en. Data were collected at ambient temperature and operating frequencies of 186.5 and 400.1 MHz for ^{119}Sn and ^1H NMR spectra, respectively.

columns $c-e$ of Table 1 correspond to comparison of Sn–Sn bond lengths in three experimentally characterized crystallographic modifications of $[\text{K}(2,2,2\text{-crypt})]_3\text{Sn}_9$ and DFT-calculated gas-phase structures of HSn_9^{3-} and Sn_9^{3-} . The DFT structures of the Sn_9^{3-} radical²⁶ and the diamagnetic HSn_9^{3-} cluster have very similar Sn_9 cores that differ only slightly in the Sn1–Sn3 and Sn2–Sn4 diagonal distances. While the metric parameters of structure A seem to be more akin to those of the calculated for Sn_9^{3-} , structures B and C are intermediate to those of the calculated HSn_9^{3-} and the Sn_9^{3-} structures (Table 1). Unfortunately, the differences are small and the analyses can be interpreted in different ways (e.g., crystal packing effects, variable mixtures of HSn_9^{3-} and Sn_9^{3-} , etc.). As such, even the combination of XRD studies and DFT calculations cannot effectively differentiate between the paramagnetic Sn_9^{3-} radical and the diamagnetic HSn_9^{3-} in a conclusive manner.

The $[\text{K}(2,2,2\text{-crypt})]_6[\text{Ni}@\text{HSn}_9]_2\text{tol}\cdot 3\text{en}$ salt is monoclinic, space group $P2_1/c$, and contains two independent $\text{Ni}@\text{HSn}_9^{3-}$ clusters that form solid solutions with HSn_9^{3-} ions (i.e., $\text{Ni}@\text{HSn}_9^{3-}$ and HSn_9^{3-} cocrystallize). Figure 1c shows the structure of the $\text{Ni}@\text{HSn}_9^{3-}$ ion obtained from pure $[\text{K}(2,2,2\text{-crypt})]_6[\text{Ni}@\text{HSn}_9]_2\text{tol}\cdot 3\text{en}$ salt that did not contain HSn_9^{3-} impurities. The $\text{Ni}@\text{HSn}_9^{3-}$ ion has a distorted tricapped trigonal prismatic structure that is quite similar to

the parent HSn_9^{3-} cluster and the isoelectronic $\text{Cu}@\text{Sn}_9^{3-}$.²⁷ Both ions are nine-vertex, 22-electron clusters in a Wade–Mingos-type analysis. The Sn_9 core of the $\text{Ni}@\text{HSn}_9^{3-}$ ion is slightly expanded relative to that of the HSn_9^{3-} ion, with two major elongations of the Sn1–Sn3 and Sn5–Sn6 prism heights (Figure 1). The position of the hydrogen atom was calculated using DFT with the lowest energy structure shown in Figure 1d. The bridge position is quite similar to that of the bridging SnCy_3 substituent in the isoelectronic $\text{Pd}@\text{Sn}_9\text{SnCy}_3^{3-}$ cluster.²⁸ Details of the solid-state structure and DFT calculations can be found in the Supporting Information. The NMR data for the $\text{Ni}@\text{HSn}_9^{3-}$ ion was reported previously,²⁹ and during the initial preparation of this manuscript, the structure of the $\text{Ni}@\text{HSn}_9^{3-}$ ion was reported.³⁰ The present structural analysis contains fully occupied Ni interstitials and identifies the location of the hydrogen atom.

NMR Studies. The ^1H and ^{119}Sn NMR spectra for a crystalline sample of the $[\text{K}(2,2,2\text{-crypt})]_3\text{HSn}_9$ and $[\text{K}(2,2,2\text{-crypt})]_6[\text{Ni}@\text{HSn}_9]_2\text{tol}\cdot 3\text{en}$ salts dissolved in en prove the diamagnetic nature of the compounds as well as the presence of a hydrogen atom attached to the Sn_9 core in these clusters. These data are presented below.

Despite the virtual C_s point symmetry of the cluster, the HSn_9^{3-} ion gives a single time-averaged ^{119}Sn NMR resonance due to a facile diamond-square-diamond intramolecular

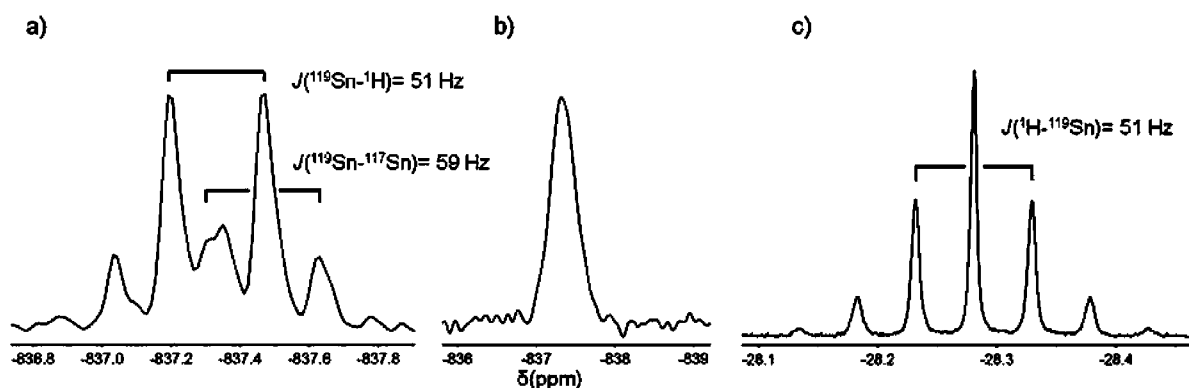


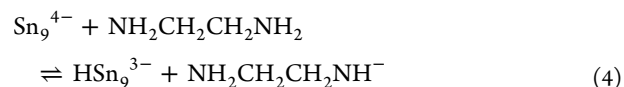
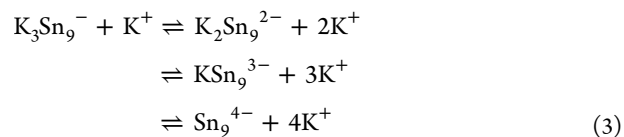
Figure 3. (a) ^{119}Sn NMR, (b) $\{^1\text{H}\}^{119}\text{Sn}$ NMR, and (c) ^1H NMR spectra of the $\text{Ni}@\text{HSn}_9^{3-}$ ion. The data were recorded from a crystalline sample of the $[\text{K}(2,2,2\text{-crypt})]_6[\text{Ni}@\text{HSn}_9]_2 \cdot \text{tol} \cdot 3\text{en}$ dissolved in $\text{py}-d_5$. Data were collected at ambient temperature and operating frequencies of 186.5 and 500.1 MHz for ^{119}Sn and ^1H NMR spectra, respectively.

exchange of all nine Sn atoms that is commonly observed in most Sn_9 clusters.²⁹ Unlike the resonances observed for the $\text{K}_x\text{Sn}_9^{(4-x)-}$ ions described below, the ^{119}Sn NMR resonance for HSn_9^{3-} is a doublet with a small $J(^{119}\text{Sn}-^1\text{H}) = 21$ Hz coupling due to intramolecular coupling to the proton. For reference, one-bond $^{119}\text{Sn}-^1\text{H}$ coupling constants in organostannanes are typically quite large (e.g., $J(^{119}\text{Sn}-^1\text{H}) = 1609$ Hz HSnBu_3)³¹ and are >80 Hz even when bridging two Sn atoms.³² The proton resonance for HSn_9^{3-} appears at 6.18 ppm in the ^1H NMR spectrum and shows $J(^{119}\text{Sn}-^1\text{H})$ coupling and $^{119}/^{117}\text{Sn}$ satellites characteristic²⁹ of coupling to nine equivalent Sn atoms (Figure 2). The single ^{119}Sn chemical shift and the equivalent coupling between the proton and all nine Sn atoms indicate that the H atom rapidly scrambles across the Sn_9 cluster in an intramolecular fashion. While proton scrambling has been seen in related transition metal hydride clusters,³³ the facile hydrogen migration in HSn_9^{3-} is quite surprising in view of the static nature of the R–Sn bond in the closely related RSn_9^{3-} ions (R = *t*-Bu, *i*-Pr)^{20,29} and the lack of such behavior in organostannanes. The $J(^{119}\text{Sn}-^{117}\text{Sn}) = 398$ Hz coupling is large relative to other RSn_9^{3-} ions, which suggests a more closed transition state that accompanies a mobile *exo* substituent.^{20a}

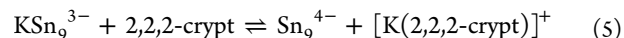
The NMR spectra for the $\text{Ni}@\text{HSn}_9^{3-}$ ion are similar to those of HSn_9^{3-} and are also diagnostic of a highly fluxional Sn_9 core with a hydride ligand that rapidly migrates around the cluster in an intramolecular fashion (Figure 3). The major differences between the two sets of spectra are the upfield hydride-like ^1H NMR chemical shift of the $\text{Ni}@\text{HSn}_9^{3-}$ hydride ligand ($\delta = -28.3$ ppm) and the larger $^{119}/^{117}\text{Sn}-^1\text{H}$ coupling constant of 51 Hz. The ^{119}Sn NMR signal is shifted to -837 ppm with a $^{119}\text{Sn}-^{117}\text{Sn}$ coupling of 59 Hz. This coupling is consistent with an expanded Sn_9 core and indicative of an endohedral $\text{M}@\text{Sn}_9$ complex.²⁹

Equilibrium Studies. The HSn_9^{3-} ion is formed through an equilibrium process involving deprotonation of the en solvent. Intermetallic melts of nominal composition K_4Sn_9 dissolve in en solvents to give solutions of $\text{K}_x\text{Sn}_9^{(4-x)-}$ ions where $x = 0, 1, 2, 3$ and HSn_9^{3-} according to eqs 3 and 4. Ion association between alkali ions and the E_9^{4-} ions (E = Ge, Sn, Pb) has been well established through the NMR experiments of Rudolph and co-workers.³⁴ Their studies revealed that the $\text{A}_x\text{Sn}_9^{(4-x)-}$ ions (A = Na, K, Rb, Cs) give rise to single, time-averaged ^{119}Sn NMR chemical shifts that have significant alkali ion dependence due to strong ion pairing in en. For example,

the time averaged ^{119}Sn NMR chemical shifts of A_xSn_9 salts span 108 ppm from $\delta = -1223$ ppm (Na_4Sn_9) to -1115 ppm (Cs_4Sn_9).^{29,34} Because the Sn_9^{4-} ion has a very high affinity for alkali ions, equilibrium 3 is shifted significantly to the left to give a preponderance of $\text{K}_3\text{Sn}_9^{3-}$ as the major Sn_9 species in solution, as described below and in the Supporting Information.



Addition of 2,2,2-crypt to these solutions results in the sequestration of the K^+ ions to give the well-known $\text{K}(2,2,2\text{-crypt})^+$ complex that has large formation constants in a variety of solvents ($K_{\text{crypt}} \geq 10^6$ in en, see Supporting Information).³⁵ Potassium ion sequestration through the addition of ≥ 4 equiv of 2,2,2-crypt shifts equilibrium 3 to the right to give $\text{K}_2\text{Sn}_9^{2-}$, KSn_9^{3-} , and Sn_9^{4-} in solution. NMR titration studies show systematic changes in the ^{119}Sn NMR chemical shifts of the $\text{K}_x\text{Sn}_9^{(4-x)-}$ species (Figure 4) when 2,2,2-crypt is added that results in a limiting chemical shift of -1236 ppm. Addition of 4.5–7.5 equiv of 2,2,2-crypt does not effect additional change in the chemical shift but instead causes significant broadening of the peak and the appearance of the HSn_9^{3-} resonance at -1268 ppm. Importantly, HSn_9^{3-} is not in rapid exchange with the $\text{K}_x\text{Sn}_9^{(4-x)-}$ species or $\text{NH}_2\text{CH}_2\text{CH}_2\text{NH}^-$ on the NMR time scale; i.e., proton coupling is maintained and the ^{119}Sn resonance for HSn_9^{3-} does not broaden with the added 2,2,2-crypt (Figure 4). These data suggest that equilibrium 3 is shifted toward the right with ≥ 4 equiv of 2,2,2-crypt but K^+ , Sn_9^{4-} contact ion pairing persists under these conditions. The broadening of the -1236 ppm resonance and the titration behavior seem most consistent with a K^+ ion exchange process, such as eq 5, that is accelerated by the addition of 2,2,2-crypt.



The broadness of the -1236 ppm resonance shows that at least two species are in equilibrium (e.g., KSn_9^{3-} and Sn_9^{4-}) and suggests that Sn_9^{4-} is not the predominant cluster in solution. The small $\sim 10\%$ increase in HSn_9^{3-} concentration observed when the 2,2,2-crypt concentration is increased from

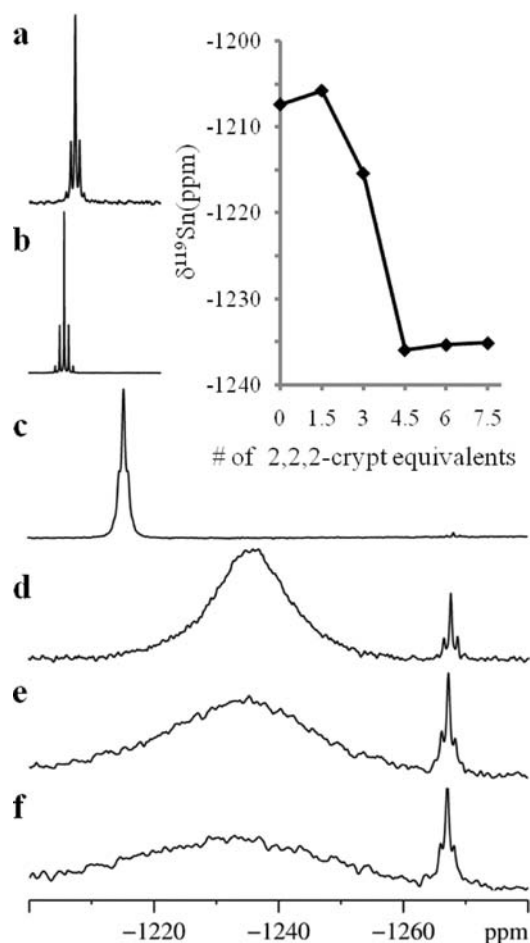
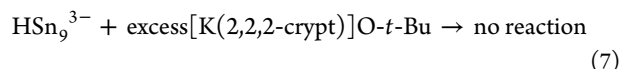
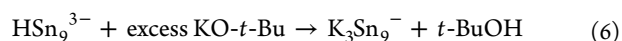


Figure 4. ^{119}Sn NMR spectra showing titrations of 0.041 M en solutions of K_4Sn_9 with 2,2,2-crypt. ^{119}Sn NMR spectra of K_4Sn_9 in en with the following 2,2,2-crypt: K_4Sn_9 ratios: (a) no 2,2,2-crypt, (b) 1.5:1, (c) 3:1, (d) 4.5:1, (e) 6:1, (f) 7.5:1. Inset: Plot of $\delta^{119}\text{Sn}$ (ppm) vs 2,2,2-crypt equivalents.

4 to 7.5 equiv shows that equilibrium 3 continues to shift to the right and suggests that the Sn_9^{4-} formed is converted to HSn_9^{3-} . Although an exact binding constant cannot be directly calculated due to the competing reaction 4, it is clear that $\text{K}_x\text{Sn}_9^{(4-x)-}$ species persist in the presence of excess 2,2,2-crypt, and, therefore, Sn_9^{4-} apparently has a very large K^+ binding constant comparable to that of 2,2,2-crypt in en.³⁵ The isolation of only $\text{K}^+\text{Sn}_9^{4-}$ ion-paired coordination complexes^{10–12} and the absence of free Sn_9^{4-} structures containing K^+ , Rb^+ , and Cs^+ ions are also consistent with extremely large formation constants for binding the “softer” alkali ions.²⁶ While HSn_9^{3-} is the minor component in the equilibrium mixture with 7.5 equiv of 2,2,2-crypt ($\text{HSn}_9^{3-}/\text{KSn}_9^{3-} = 1:10$ by NMR integration), it crystallizes as the $[\text{K}(2,2,2\text{-crypt})]^+$ salt in high yields due to its lower solubility relative to the other species in solution and its continual replenishment due to a Le Châtelier-type equilibrium shift.

The equilibrium shift caused by addition of 2,2,2-crypt is completely reversible, such that addition free K^+ ions and a strong base will shift eq 3 back to the left. For example, addition of KCl to the equilibrium mixture of $\text{HSn}_9^{3-}/\text{NH}_2\text{CH}_2\text{CH}_2\text{NH}^-$ above quantitatively shifts the equilibria 1 and 2 back to K_3Sn_9^- and en, as shown in Figure S1. Likewise, en solutions of HSn_9^{3-} prepared from crystalline samples of

$[\text{K}(2,2,2\text{-crypt})]_3\text{HSn}_9 \cdot 1.5\text{en}$ are converted to K_3Sn_9^- and $t\text{-BuOH}$ upon reaction with excess $\text{KO-}t\text{-Bu}$ according to eq 6 (Figure S2). However, addition of just a base to these solutions without free potassium ions (e.g., $[\text{K}(2,2,2\text{-crypt})]\text{O-}t\text{-Bu}$) does not change the position of the equilibrium (eq 7), which indicates that the pK_a of HSn_9^{3-} in en is greater than that of $t\text{-BuOH}$ [$\text{pK}_a(\text{dmsO}) \approx 32$]³⁶ in the absence of K^+ ion association. Moreover, the addition of free K^+ ions in the absence of a strong base results in a slow degradation of the HSn_9^{3-} cluster, giving only trace amounts of $\text{K}_x\text{Sn}_9^{(4-x)-}$ and other unidentified species.



To quantify the concentration of HSn_9^{3-} in the crystalline samples of $[\text{K}(2,2,2\text{-crypt})]_3\text{HSn}_9 \cdot 1.5\text{en}$, we performed quantitative deprotonation experiments (eq 6) in the presence of an internal reference (Rb_4Sn_9 in a capillary). Crystals of $[\text{K}(2,2,2\text{-crypt})]_3\text{HSn}_9 \cdot 1.5\text{en}$ were dissolved in en solvent and charged with excess $\text{KO-}t\text{-Bu}$. Repeated experiments from various crystalline samples showed between 75% and 90% conversion to the K_3Sn_9^- ion (82% ave, see Figure S4). Since $\text{KO-}t\text{-Bu}$ is a Brønsted base and not a reducing agent, these experiments show that crystalline samples of $[\text{K}(2,2,2\text{-crypt})]_3\text{HSn}_9 \cdot 1.5\text{en}$ dissolve to give solutions of HSn_9^{3-} as the major component.

Because the titrations above did not give quantitative conversions to the K_3Sn_9^- ion, we also evaluated the concentration of paramagnetic species in en solutions of $[\text{K}(2,2,2\text{-crypt})]_3\text{HSn}_9 \cdot 1.5\text{en}$ by way of the Evan’s method. Concentration-dependent shifts of reference peak (benzene) were measured against an internal reference sealed in a capillary in the traditional manner, except the internal reference was charged with an isomolar concentration of 2,2,2-crypt to minimize the diamagnetic correction. The data showed low concentrations of paramagnetic species that varied from sample to sample (Figure S5).

The results described above can be rationalized as follows. The Brønsted basicities of the $\text{K}_x\text{Sn}_9^{(4-x)-}$ ions (where $x = 1, 2, 3$), which contain direct contact ion pairs $\text{K}^+\text{Sn}_9^{4-}$, are significantly less than that of the “free ion” Sn_9^{4-} , and they do not deprotonate ethylenediamine or $t\text{-BuOH}$ in en or dmf to any noticeable extent. Similar ion-pairing-induced changes in Brønsted basicity and the effect of cryptand additives have been well documented for organic bases that bind alkali ions.^{37,38}

Crystalline samples of $[\text{K}(2,2,2\text{-crypt})]_3\text{HSn}_9$ dissolved in dmf and pyridine do not show ^{119}Sn NMR signals, even at low temperatures. However, addition of $\text{KO-}t\text{-Bu}$ to these solutions results in the formation of K_3Sn_9^- in high concentrations (Figure S2), suggesting that HSn_9^{3-} was indeed present but is not detectable by NMR. In contrast, addition of $[\text{K}(2,2,2\text{-crypt})]\text{O-}t\text{-Bu}$ has no effect on the solution, indicating that K^+ and base are necessary to deprotonate HSn_9^{3-} as discussed above. We believe that the acid/base and dynamic exchange processes may be fast on the NMR time scale in these solvents and, perhaps in combination with trace impurities, broaden the ^{119}Sn NMR signals beyond detection.

DISCUSSION

We have shown that the Sn_9^{4-} ion is both a potent potassium-ion sequestering agent that competes with 2,2,2-crypt in en solutions and a very strong Brønsted base with a K_3 similar to

that of the amide anion $\text{NH}_2\text{CH}_2\text{CH}_2\text{NH}^-$. The HSn_9^{3-} ion exhibits fluxionality of the Sn_9 cage that is quite typical of this class of compounds but the rapid intramolecular proton scrambling is quite surprising. NMR data suggest that the HSn_9^{3-} and $\text{K}_x\text{Sn}_9^{(4-x)-}$ ions (where $x = 1, 2, 3$) are the predominant species in en solutions regardless of conditions; however, the Sn_9^{4-} ion clearly exists in solution as evidenced by its isolation in two different crystal structures.^{4,7} While this HSn_9^{3-} cluster is the likely precursor to most Sn_9 derivatives reported to date, it has escaped detection due to the complicated acid/base equilibria and dynamic exchange processes that hinder traditional NMR characterization.

The nature of the Sn_9^{3-} radical anion is less clear. The chemistries described here are clearly acid/base reactions and classical ion binding that are entirely consistent with the $\text{S}_\text{N}2$ -type alkylation chemistry established for this class of compounds.²¹ Moreover, the acid/base chemistry is highly reminiscent of the $\text{P}_7^{3-}/\text{HP}_7^{2-}$ compounds and their metalated derivatives.^{39–43} In addition, the reported¹⁶ incomplete paramagnetism of the Sn_9^{3-} ions and the difficulty in observing solution EPR signals with characteristic $^{119}\text{Sn}/^{117}\text{Sn}$ hyperfine couplings that accompany $S = 1/2$ Sn_9 clusters⁴⁴ are also suggestive that the previous studies involved significant concentrations of the diamagnetic HSn_9^{3-} ions. The titration studies of the $[\text{K}(2,2,2\text{-crypt})]_3[\text{HSn}_9]\cdot\text{en}_{1.5}$ crystalline samples dissolved in en or dmf strongly suggest that the HSn_9^{3-} ion is the predominant cluster in solution. However, our solution magnetic susceptibility studies, along with previous solid-state susceptibility studies,¹⁶ also show low concentrations of paramagnetic species that could be a signature of the Sn_9^{3-} radical anion. While it is possible that HSn_9^{3-} and the Sn_9^{3-} radical coexist in solution and in the solid state, we believe that the previously reported salts of Sn_9^{3-} radical anion as well as the E_9^{3-} anions ($\text{E} = \text{Si}, \text{Ge}, \text{Pb}$) most likely contain the protonated HE_9^{3-} analogues of HSn_9^{3-} . The similarities in electronegativities of Ge, Si, and Sn suggest that HGe_9^{3-} and HSi_9^{3-} clusters should also exist, but the NMR studies involving these nuclei are more challenging.

EXPERIMENTAL SECTION

General. All reactions were performed in a nitrogen atmosphere drybox. Melts of nominal composition K_4Sn_9 were made by fusion of stoichiometric ratios of the elements in silica tubes at high temperature under N_2 atmosphere. The chemicals were heated carefully with a natural gas/oxygen flame. **Caution!** Molten alloy synthesis can result in serious explosion, and reactions should be conducted with great caution behind blast shields. 4,7,13,16,21,24-Hexaoxa-1,10-diazobicyclo[8,8,8]-hexacosane (2,2,2-crypt) were purchased from Fisher Scientific and kept under vacuum for 2 days. Anhydrous ethylenediamine (en), dimethylformamide (dmf), and deuterated pyridine (py) were purchased from Fisher; en and dmf were vacuum-distilled from K_4Sn_9 and stored under dinitrogen. Deuterated pyridine was distilled from KOH under dinitrogen and stored under dinitrogen. Toluene was distilled from sodium/benzophenone under dinitrogen and stored under dinitrogen. KCl was purchased from J.T. Baker and dried under vacuum. K-O-*t*-Bu was purchased from Sigma-Aldrich and vacuum-dried for 24 h. $\text{Ni}(\text{cod})_2$ was purchased from STREM chemicals. The percentage yields for the crystalline HSn_9^{3-} and $\text{Ni}@\text{HSn}_9^{3-}$ ions were based on K_4Sn_9 used.

$\text{K}(2,2,2\text{-crypt})^+$ Formation Constants. The equilibrium stability constants for the formation of the $\text{K}(2,2,2\text{-crypt})^+$ have been studied in several solvents including water, dmf, EtOH, and acetonitrile. The smallest stability constants ($\log K_s$) are for water (5.5), DMSO (7.0), and dmf (7.9).³⁵ Based on these data, we estimate that K_s in en is ≥ 6.0 .

^{119}Sn and ^1H NMR Experiments. All NMR samples were prepared in a nitrogen atmosphere. The NMR solutions of the crystalline samples were prepared by grinding single crystals of $[\text{K}(2,2,2\text{-crypt})]_3[\text{HSn}_9]\cdot\text{en}_{1.5}$ and extracting the powder in en. The ^1H NMR spectrum of HSn_9^{3-} was recorded on a Bruker AVANCE 400 instrument operating at 400.1 MHz with Broad Band Inverse probe. In this experiment, a 90° Gaussian shaped pulse of 2 ms with excitation bandwidth of 1061 Hz was applied at 6 ppm, which is in the proximity of the ^1H signal of interest. Thus, the proton signal of HSn_9^{3-} at 6.18 ppm was semiselectively excited with a slight suppression of the other signals. For ^1H chemical shift calibration, the central signal of the para proton of the residual toluene was set at 7.16 ppm. The ^1H NMR spectrum for $[\text{K}(2,2,2\text{-crypt})]_6[\text{Ni}@\text{HSn}_9]_2\cdot\text{tol}\cdot\text{en}_3$ was recorded from a py- d_5 solution on a Bruker DRX500 AVANCE instrument operating at 500.1 MHz. The ^1H NMR chemical shifts were referenced to the py- d_5 signal at 8.74 ppm. The ^{119}Sn NMR spectra for both ions were recorded on a Bruker DRX500 AVANCE spectrometer at 186.5 MHz. The pulse sequence used for the ^{119}Sn NMR studies was the standard Bruker pulse program with a 90° pulse and 0.3 s relaxation delay. A total of 300 dummy scans were used for each ^{119}Sn NMR experiment. The signals were confirmed and verified by repeating the final measurements with different transmitter offsets. The ^{119}Sn chemical shifts were referenced to an external Me_4Sn standard in C_6D_6 (0 ppm) at room temperature.

Titration of K_4Sn_9 with 2,2,2-Crypt. For the titration of the en solutions of K_4Sn_9 with 2,2,2-crypt, 40 mg of K_4Sn_9 (0.033 mmol) was dissolved in 0.8 mL of en solvent in a glass vial to give a 0.041 M solution. Residual insoluble intermetallics from the K_4Sn_9 extractions were removed by filtration and not included in the calculations of concentrations. After each NMR experiment, the NMR sample was taken in the glovebox and increments of 2,2,2-crypt (18.4 mg, 0.049 mmol) were sequentially added to the solution to give the data in Figure 4. Three independent titration experiments were conducted and gave very similar results. Addition of NH_4Cl to the solutions increased the relative concentrations of HSn_9^{3-} in all cases, provided that at least 4 equiv of 2,2,2-crypt were present.

Conversion of HSn_9^{3-} to K_3Sn_9^- . The K_4Sn_9 solution containing 7.5 equiv of 2,2,2-crypt shown in Figure S1a (and Figure 4f) was charged with anhydrous KCl (0.15 g, 2 mmol). The solution was stirred for 15 min and filtered through tightly packed glass wool. The resulting ^{119}Sn NMR spectrum of the reaction mixture is shown in Figure S1b.

Deprotonation Experiments for Estimation of $\text{p}K_a$ of the HSn_9^{3-} Ion in en. $[\text{K}(2,2,2\text{-crypt})]_3[\text{HSn}_9]\cdot\text{en}_{1.5}$ (37 mg, 0.015 mmol) was dissolved in en (0.8 mL). Anhydrous K-O-*t*-Bu (5.5 mg, 0.049 mmol) was added as solid to this solution. ^{119}Sn NMR spectra before and after the reaction are shown in Figure S2a,b. Subsequently, 2,2,2-crypt (6 mg, 0.016 mmol) and anhydrous K-O-*t*-Bu (1.7 mg, 0.015 mmol) were added as solid to the solution shown in Figure S2a; the spectrum is shown in Figure S2c.

Deprotonation Experiments of the HSn_9^{3-} Ion in dmf. The ^{119}Sn NMR spectra of K_4Sn_9 (60 mg, 0.049 mmol) in dmf (0.8 mL) and the crystalline sample of $[\text{K}(2,2,2\text{-crypt})]_3[\text{HSn}_9]\cdot\text{en}_{1.5}$ (75 mg, 0.031 mmol) in dmf (0.8 mL) solution are shown in Figure S3a,b. In a separate experiment, K-O-*t*-Bu (15 mg, 0.13 mmol) and 2,2,2-crypt (50 mg, 0.13 mmol) were dissolved in 0.2 mL of dmf. This solution was added to a dmf solution containing the crystalline sample of $[\text{K}(2,2,2\text{-crypt})]_3[\text{HSn}_9]\cdot\text{en}_{1.5}$ (56 mg, 0.023 mmol) (eq 6). The ^{119}Sn NMR spectrum after the reaction is shown in Figure S3c. To the sample in Figure S3b was added K-O-*t*-Bu (20 mg, 0.18 mmol) as a solid (eq 7), and the ^{119}Sn NMR spectrum was recorded (Figure S4d).

Structure Determination of $[\text{K}(2,2,2\text{-crypt})]_3[\text{HSn}_9]\cdot\text{en}_{1.5}$. A black plate of $\text{C}_{57}\text{H}_{120}\text{K}_3\text{N}_9\text{O}_{18}\text{Sn}_9$, approximate dimensions $0.26 \times 0.38 \times 0.49 \text{ mm}^3$, was used for the X-ray crystallographic analysis. The X-ray intensity data were measured at 100(2) K on a three-circle diffractometer system equipped with Bruker Smart Apex II CCD area detector using a graphite monochromator and a Mo $K\alpha$ fine-focus sealed tube ($\lambda = 0.71073 \text{ \AA}$). The detector was placed at a distance of 5.000 cm from the crystal.

The structure was solved and refined using the SHELXS-97 and SHELXL-97 software^{45,46} in the space group $P\bar{1}$ with $Z = 2$ for the formula unit $C_{57}H_{120}K_3N_9O_{18}Sn_9$. The final anisotropic full-matrix least-squares refinement on F^2 with 897 variables converged at $R_1 = 3.45\%$ for the observed data and $wR_2 = 7.28\%$ for all data. The goodness-of-fit was 1.000. The largest peak on the final difference map was $4.036 \text{ e}^-/\text{\AA}^3$, and the largest hole was $-1.672 \text{ e}^-/\text{\AA}^3$. On the basis of the final model, the calculated density was 1.807 g/cm^3 and $F(000)$, 2352 e^- .

Structure Determination of $[\text{K}(2,2,2\text{-crypt})]_6[\text{Ni}(\text{HSn}_9)_2\text{tol}\cdot\text{en}]_3$. A red plate of $C_{121}H_{248}K_6N_{18}Ni_2O_{36}Sn_{18}$, approximate dimensions $0.042 \times 0.319 \times 0.49 \text{ mm}^3$, was used for the X-ray crystallographic analysis. The X-ray intensity data were measured at 150(2) K on a three-circle diffractometer system equipped with Bruker Smart Apex II CCD area detector using a graphite monochromator and a Mo $K\alpha$ fine-focus sealed tube ($\lambda = 0.71073 \text{ \AA}$). The detector was placed at a distance of 6.000 cm from the crystal.

The structure was solved and refined using the SHELXS-97 and SHELXL-97 software^{45,46} in the space group $P2_1/c$ with $Z = 4$ for the formula unit $C_{121}H_{248}K_6N_{18}Ni_2O_{36}Sn_{18}$. The final anisotropic full-matrix least-squares refinement on F^2 with 2156 variables converged at $R_1 = 4.17\%$ for the observed data and $wR_2 = 9.61\%$ for all data. The goodness-of-fit was 1.066. The largest peak on the final difference map was $2.519 \text{ e}^-/\text{\AA}^3$ and the largest hole was $-1.805 \text{ e}^-/\text{\AA}^3$. On the basis of the final model, the calculated density was 1.810 g/cm^3 and $F(000)$, 9832 e^- .

The crystal structure consists of six symmetrically independent K-crypt ions, two NiSn_9 clusters, one toluene (tol), and three ethylenediamine (en) solvent molecules as follows from the moiety formula $(\text{KC}_{18}\text{H}_{36}\text{N}_2\text{O}_6)_6[\text{NiSn}_9]_2(\text{C}_7\text{H}_8\text{N}_2)_3(\text{C}_2\text{H}_8\text{N}_2)_3$. Both NiSn_9 clusters are disordered in two orientations related to each other by rotation around the Ni1–Sn11 and Ni3–Sn31 axes. The ratio of disordered components was refined to 70:30 and 85:15 for Ni1 and Ni3 clusters, respectively. Occupation factors of both Ni centers were refined to 1 within the error and were considered fully occupied in the final refinement. The disorder of the Ni1 cluster could involve more than two orientations as Sn17 and Sn27 atoms from both orientations clearly show additional splitting (Sn57, Sn67). The additional splitting, however, was not noticed for other atoms of this cluster, probably due to its small magnitude. In order to decrease correlation during refinement, the atomic displacement parameters for Sn atoms from different orientations that were very close to each other were constrained to be the same, and the whole cluster was restrained to rigid-body motions. However, atomic coordinates were refined, yielding nearly the same geometry of the disordered clusters. Interestingly, only one of the six K-crypt is disordered in two orientations in a 2:1 ratio with K atom remaining in the same position. All three independent en solvent molecules are also disordered in various ratio in different orientations or conformation. However, tol solvent is not disordered within the accuracy of refinement, yet it shows somewhat enlarged ellipsoids. All atomic displacement ellipsoids of disordered ions and solvent molecules were restrained to conform with rigid-body motions and to be physically sensible.

■ ASSOCIATED CONTENT

📄 Supporting Information

Detailed experimental discussion, NMR data, computational experimental details and results, structural comparisons, and crystallographic details. This material is available free of charge via the Internet at <http://pubs.acs.org>.

■ AUTHOR INFORMATION

Corresponding Author

eichhorn@umd.edu

Notes

The authors declare no competing financial interest.

■ ACKNOWLEDGMENTS

This material is based upon work supported by the National Science Foundation under Grant No. 0401850.

■ REFERENCES

- (1) Kraus, C. A. *J. Am. Chem. Soc.* **1907**, *29*, 1557–1571.
- (2) Zintl, E.; Goubeau, J.; Dullenkopf, W. *Z. Phys. Chem. Abt. A* **1931**, *154*, 1–46.
- (3) Diehl, L.; Khodadadeh, K.; Kummer, D.; Strähle, J. *Chem. Ber.* **1976**, *109*, 3404.
- (4) Corbett, J. D.; Edwards, P. A. *J. Am. Chem. Soc.* **1977**, *99*, 3313–3317.
- (5) Wade, K. *Chem. Br.* **1975**, *11*, 177–183.
- (6) Mingos, D. M. P. *Nature Phys. Sci.* **1972**, *236*, 99–102.
- (7) Korber, N.; Fleischmann, A. *J. Chem. Soc., Dalton Trans.* **2001**, 383–385.
- (8) Scharfe, S.; Fassler, T. F. *Philos. Trans. R. Soc. A-Math. Phys. Eng. Sci.* **2010**, *368*, 1265–1284.
- (9) Scharfe, S.; Kraus, F.; Stegmaier, S.; Schier, A.; Fassler, T. F. *Angew. Chem., Int. Ed.* **2011**, *50*, 3630–3670.
- (10) Burns, R. C.; Corbett, J. D. *Inorg. Chem.* **1985**, *24*, 1489–1492.
- (11) Fassler, T. F.; Hoffmann, R. *Angew. Chem., Int. Ed.* **1999**, *38*, 543–546.
- (12) Ugrinov, A.; Sevov, S. C. *Appl. Organomet. Chem.* **2003**, *17*, 373–376.
- (13) Critchlow, S. C.; Corbett, J. D. *J. Am. Chem. Soc.* **1983**, *105*, 5715–5716.
- (14) Fassler, T. F.; Hunziker, M. *Z. Anorg. Allg. Chem.* **1996**, *622*, 837–844.
- (15) Fassler, T. F.; Hoffmann, R. *Z. Kristallogr.-New Cryst. Struct.* **2000**, *215*, 139–142.
- (16) Fassler, T. F.; Hunziker, M.; Spahr, M. E.; Lueken, H.; Schilder, H. *Z. Anorg. Allg. Chem.* **2000**, *626*, 692–700.
- (17) Yong, L.; Hoffmann, S. D.; Fassler, T. F. *Z. Kristallogr.-New Cryst. Struct.* **2005**, *220*, 49–52.
- (18) Birchall, T.; Burns, R. C.; Devereux, L. A.; Schrobilgen, G. J. *Inorg. Chem.* **1985**, *24*, 890–894.
- (19) Chapman, D.; Sevov, S. C. *Inorg. Chem.* **2008**, *47*, 6009–4014.
- (20) (a) Kocak, F. S.; Zavalij, P. Y.; Lam, Y. F.; Eichhorn, B. W. *Chem. Commun.* **2009**, 4197–4199. (b) Schrenk, C.; Neumaier, M.; Schnepf, A. *Inorg. Chem.* **2012**, *51*, 3989.
- (21) Hull, M. W.; Sevov, S. C. *J. Am. Chem. Soc.* **2009**, *131*, 9026–9037.
- (22) Perdew, J. P.; Burke, K.; Ernzerhof, M. *Phys. Rev. Lett.* **1996**, *77*, 3865–3868.
- (23) JAGUAR, Version 7.8; Schrödinger, Inc.: Portland, OR, 2011.
- (24) Laikov, D. N. *Chem. Phys. Lett.* **1997**, *281*, 151–156.
- (25) Laikov, D. N.; Ustynyuk, Y. A. *Russ. Chem. Bull.* **2005**, *54*, 820–826.
- (26) Fassler, T. F. *Coord. Chem. Rev.* **2001**, *215*, 347–377.
- (27) Scharfe, S.; Fassler, T. F.; Stegmaier, S.; Hoffmann, S. D.; Ruhland, K. *Chem.-Eur. J.* **2008**, *14*, 4479–4483.
- (28) Kocak, F. S.; Zavalij, P.; Eichhorn, B. *Chem.-Eur. J.* **2011**, *17*, 4858–4863.
- (29) Kocak, F. S.; Eichhorn, B. In *Structure and Bonding (Berlin)*; Fassler, T., Ed.; Springer-Verlag: Berlin/Heidelberg, 2011.
- (30) Rios, D.; Gillett-Kunnath, M. M.; Taylor, J. D.; Oliver, A. G.; Sevov, S. C. *Inorg. Chem.* **2011**, *50*, 2373–2377.
- (31) Maddox, M. L.; Flitcrof, N.; Kaesz, H. D. *J. Organomet. Chem.* **1965**, *4*, 50–56.
- (32) Rivard, E.; Fischer, R. C.; Wolf, R.; Peng, Y.; Merrill, W. A.; Schley, N. D.; Zhu, Z. L.; Pu, L.; Fetting, J. C.; Teat, S. J.; Nowik, I.; Herber, R. H.; Takagi, N.; Nagase, S.; Power, P. P. *J. Am. Chem. Soc.* **2007**, *129*, 16197–16208.
- (33) Kesanli, B.; Halsig, J. E.; Zavalij, P.; Fetting, J. C.; Lam, Y.-F.; Eichhorn, B. W. *J. Am. Chem. Soc.* **2007**, *129*, 4567–4574.
- (34) Wilson, W. L.; Rudolph, R. W.; Lohr, L. L.; Taylor, R. C.; Pyykko, P. *Inorg. Chem.* **1986**, *25*, 1535–1541.

- (35) Cox, B. G.; Garciarosas, J.; Schneider, H. *J. Am. Chem. Soc.* **1981**, *103*, 1384–1389.
- (36) Bordwell, F. G.; Drucker, G. E.; Fried, H. E. *J. Org. Chem.* **1981**, *46*, 632–635.
- (37) Antipin, I. S.; Gareyev, R. F.; Vedernikov, A. N.; Kononov, A. I. *J. Phys. Org. Chem.* **1994**, *7*, 181–191.
- (38) Bordwell, F. G. *Acc. Chem. Res.* **1988**, *21*, 456–463.
- (39) Charles, S.; Eichhorn, B. W.; Bott, S. G.; Fettinger, J. C. *J. Am. Chem. Soc.* **1996**, *118*, 4713–4714.
- (40) Dai, F. R.; Xu, L. *Inorg. Chim. Acta* **2006**, *359*, 4265–4273.
- (41) Korber, N.; Vonschnering, H. G. *J. Chem. Soc., Chem. Commun.* **1995**, 1713–1714.
- (42) Charles, S.; Eichhorn, B. W.; Fettinger, J. C.; Bott, S. G. *Inorg. Chem.* **1996**, *35*, 1540–1548.
- (43) Baudler, M. *Angew. Chem., Int. Ed. Engl.* **1982**, *21*, 492–512.
- (44) Kesanli, B.; Fettinger, J.; Gardner, D. R.; Eichhorn, B. *J. Am. Chem. Soc.* **2002**, *124*, 4779–4786.
- (45) Sheldrick, G. M. *SHELXS-97*; Universitat Gottingen: Gottingen, Germany, 1996.
- (46) Sheldrick, G. M. *Acta Crystallogr., Sect. A* **2008**, *64*, 112–122.